Strong divergent selection at multiple loci in two closely related species of ragworts adapted to high and low elevations on Mount Etna

Wong, Edgar L Y; Nevado, Bruno; Osborne, Owen G; Papadopulos, Alexander S T; Bridle, Jon R; Hiscock, Simon J; Filatov, Dmitry A

Molecular Ecology

DOI:
10.1111/mec.15319
10.1111/mec.15319

Published: 01/01/2020

Peer reviewed version

Strong divergent selection at multiple loci in two closely related species of ragworts adapted to high and low elevations on Mount Etna

Running title: Strong selection in ragworts on Mount Etna

Edgar L.Y. Wong[1,*], Bruno Nevado[1], Owen G. Osborne[1,3], Alexander S.T. Papadopulos[1,3], Jon R. Bridle[2], Simon J. Hiscock[1] and Dmitry A. Filatov[1]

[1]Department of Plant Sciences, University of Oxford, Oxford, OX1 3RB, UK

[2]School of Biological Sciences, University of Bristol, Bristol, BS8 IUG, UK

[3]Current Address: Molecular Ecology and Fisheries Genetics Laboratory, Environment Centre Wales, School of Natural Sciences, Bangor University, Bangor, LL57 2UW, UK

*corresponding author: Edgar L.Y. Wong, edgar.wong@plants.ox.ac.uk

Abstract

Recently diverged species present particularly informative systems for studying speciation and maintenance of genetic divergence in the face of gene flow. We investigated speciation in two closely related *Senecio* species, *S. aethnensis* and *S. chrysanthemifolius*, which grow at high and low elevations, respectively, on Mount Etna, Sicily and form a hybrid zone at intermediate elevations. We used a newly generated genome-wide single nucleotide polymorphism (SNP) dataset from 192 individuals collected over 18 localities along an elevational gradient to reconstruct the likely history of speciation, identify highly differentiated SNPs, and estimate the strength of divergent selection. We found that speciation in this system involved heterogeneous and bidirectional gene flow along the genome, and species experienced marked population size changes in the past. Furthermore, we identified highly-differentiated SNPs between the species, some of which are located in genes potentially involved in ecological differences between species (such as photosynthesis and UV response). We analysed the shape of these SNPs' allele frequency clines along the elevational gradient. These clines show significantly variable coincidence and concordance, indicative of the presence of multifarious selective forces. Selection against hybrids is estimated to be very strong (0.16 – 0.78) and one of the highest reported in literature. The combination of strong cumulative selection across the genome and previously identified intrinsic incompatibilities likely work together to maintain the genetic and phenotypic differentiation between these species – pointing to the importance of considering both intrinsic and extrinsic factors when studying divergence and speciation.

Keywords

speciation, gene flow, selection, adaptation, hybrid zone

Introduction

Defining what constitutes a species and understanding how new species form are central questions in evolutionary biology. The idea that speciation is driven by adaptation to distinct environmental conditions has a long history going back to Darwin's concept of new species formation by means of natural selection. Although natural selection is the main driver of evolutionary changes, its role in creating barriers to gene flow is not well understood. Adaptation to distinct environments (divergent selection) may lead to differentiation in loci responsible for adaptation or even fixation of different alleles in isolated populations. This can generate a mosaic with different genomic regions having different extents of gene flow, and consequently, genetic divergence (Feder, Egan, & Nosil, 2012; Mallet, 2005; Teeter et al., 2008; Wu, 2001). This effect allows evolutionary biologists to study genetic and phenotypic differences between species in relation to environmental or ecological change, and in areas where populations meet, such as hybrid zones. Hybrid zones, and more generally systems in which reproductive isolation is incomplete, are powerful tools for this purpose. This is because the basis of reproductive isolation and recombinants can be more easily detected in these systems without being obscured by post-speciation divergence.

Genetic and phenotypic trait differences between species or populations can be tracked along geographical clines. Parameters of clines are informative about the strength of selection and dispersal rate (Barton & Gale, 1993; Barton & Hewitt, 1985; Szymura & Barton, 1986; 1991), while cline coincidence and concordance inform us about selective pressures in the hybrid zone. For instance, both coincidence and concordance could suggest they are influenced by their respective gradients (whether identical or different) in a similar way (Barton & Gale, 1993; Kruuk et al., 1999; Young, 1996); whereas discordant clines could

61 suggest the presence of several external selective pressures (Durrett, Buttel, & Harrison, 2000).
62 Tracking the change in allele frequency or trait values along the clines allow us to evaluate the
63 nature, magnitude and relative importance of selection in shaping the hybrid zone, thus
64 enable a deeper understanding of microevolutionary bases of local adaptation and
65 reproductive isolation. Several studies have estimated the strength of selection in different
66 systems (Table 1), with estimated selection coefficient ranging from as low as 0.0017 to over
67 0.7. Surprisingly, although interspecific hybridisation is common in plants, there is a lack of
68 selection estimates for plant hybrid zones [e.g. Antonovics & Bradshaw, 1970 (this study
69 estimated selection using a different method comapred to the one in our study); Brennan et
70 al., 2009]. Our study aims to fill this gap, providing a detailed analysis of selection maintaining
71 an altitudinal hybrid zone in *Senecio* on Mount Etna, Sicily.
72 It is thought that the chance of local adaptation leading to speciation can be increased
73 by either strong selection on a single trait or selection on a larger number of traits (stronger
74 selection and multifarious selection hypotheses; Nosil, Harmon, & Seehausen, 2009).
75 Although speciation with one or few traits have been well characterised, an increasing number
76 of cases are reporting the presence of multifarious selection in different systems. For example,
77 selection by both breeding pool acidity and predators in frogs (*Rana arvalis;* Egea-Serrano,
78 Hangartner, Laurila, & Räsänen, 2014), selection on female oviposition preference and
79 diapause initiation in butterflies (*Lycaeides* sp.; Gompert et al., 2013), selection on various
80 diapause life-history traits in flies (*Rhagoletis* sp.; Daroski & Feder, 2007), and selection on
81 floral colour and other ecophysiological traits in monkeyflowers (*Mimulus aurantiacus*; Sobel
82 et al., 2019; Stankowski et al., 2017). In cases where there is multifarious selection, although
83 selection on each trait might not be strong enough to cause speciation on its own, it is the

cumulative effect of many selective agents that leads to strong reproductive isolation and divergence overall; genetic hitchhiking leading to correlated response of many genes could also be effective in driving divergence in the multifarious selection scenario (Nosil et al., 2009).

In this study, we created clines for several genetic and phenotypic markers, and estimated the strength of selection against hybrids in an altitudinal hybrid zone in two *Senecio* (Asteraceae) species on Mount Etna, Sicily. We also reconstructed the history of their speciation and describe the interplay among demography, gene flow and selection in this system. The two study species, *Senecio aethnensis* and *Senecio chrysanthemifolius*, maintain a hybrid zone at their intermediate elevations at around 1,000 – 2,000m (Chapman, Forbes, & Abbott, 2005; James & Abbott, 2005), where they exhibit a range of intermediate phenotypes between the two species (Brennan, Bridle, Wang, Hiscock, & Abbott, 2009; James & Abbott, 2005). *S. aethnensis* and *S. chrysanthemifolius*' habitats show contrasting environmental conditions, both elevation- and ecology-related, such as temperature, solar radiation, and water availability (James & Abbott, 2005; Körner, 2007; Ross, 2010). Their divergence was estimated to have occurred less than 200,000 years ago, coinciding with the rise of Mount Etna to elevations above 2,000 m due to volcanic activity (Chapman, Hiscock, & Filatov, 2013; Muir, Osborne, Sarasa, Hiscock, & Filatov, 2013; Osborne, Batstone, Hiscock, & Filatov, 2013). Typical *S. aethnensis* occurs above 2000 m whereas typical *S. chrysanthemifolius* occurs below 1000 m (Brennan et al., 2009; Muir et al., 2013). Both species are short-lived, obligately outcrossing perennials pollinated by generalist insects and bear wind-dispersed fruits; they can be distinguished by several morphological and physiological characters, such as degree of leaf dissection, size of capitula and florets, and flowering time (Brennan et al., 2009; James & Abbott, 2005). The two species produce fertile hybrids (Chapman et al., 2005), but significant

hybrid breakdown in F_2 hybrids (Chapman, Hiscock, & Filatov, 2016), and evidence of genetic incompatibilities (Brennan, Hiscock, & Abbott, 2014; 2016; 2019; Chapman et al., 2016) suggests the two are distinct species that have evolved substantial reproductive isolation.

Previous demographic studies in this system (Filatov, Osborne, & Papadopulos, 2016; Chapman et al., 2013; Muir et al., 2013; Osborne et al., 2013) have shown the presence of low on-going gene flow between the species. It was also demonstrated that an allopatric phase during divergence of the two *Senecio* species is unlikely (Filatov et al., 2016). Other studies have identified differentially expressed genes (Chapman et al., 2013); investigated geographic clines in the Etnean *Senecio* system using phenotypic data, allozymes and simple sequence repeats, and estimated moderate selection against hybrids (0.02 - 0.41; Brennan et al., 2009); and mapped hybrid breakdown to several quantitative trait loci (Chapman et al., 2016). However, these studies have not directly tested for other demographic parameters (such as heterogeneous gene flow and population size change), patterns of gene flow within the hybrid zone, and the extent of divergent selection. In our study, we addressed these issues specifically using finer scale sampling throughout the geographical cline on the southern side of Mount Etna, combined with analysis of leaf morphology and genetic diversity based on reduced-representation genomic data ("nextRAD"; Russello, Waterhouse, Etter, & Johnson, 2015). We hypothesize that: 1) as reproductive isolation is incomplete, the two species would show demographic features of recent speciation with gene flow, such as heterogenous gene flow; 2) the system is under multifarious selection thus there would be many genetic markers under various strengths of divergent selection; and 3) there is strong cumulative selection against hybrids to maintain species divergence despite on-going gene flow. To test these hypotheses, we: 1) reconstructed the likely speciation scenario in this system, specifically

including hybrid groups and demographic models comprising parameters previously unexplored; 2) identified potential genomic targets of divergent selection and carried out cline analysis on them; and 3) estimated the strength of selection in the hybrid zone. These analyses allowed us to infer the patterns of gene flow in different parts of the hybrid zone and the extent of selection that is responsible for the maintenance of species identity and build-up of species divergence despite on-going interspecific gene flow.

Materials and Methods

Sampling

To infer the extent of genome-wide divergence between *S. aethnensis* and *S. chrysanthemifolius*, and the potential selective pressures acting on this system, we generated and analysed data comprising reduced-representation nextRAD sequences (Russello et al., 2015) and leaf dissection measurements. The same individuals were used in generating both datasets. A total of 192 individuals from 18 localities were sampled over an elevational gradient from 585 m to 2,645 m on a transect on the southern side of Mount Etna. These include six typical *S. aethnensis* (above 2,000 m) localities, three typical *S. chrysanthemifolius* (below 1,000 m) localities and nine hybrid localities (Fig. 1d); nine to 14 individuals were sampled from each locality (Table S1). Leaf material was collected and dried in silica gel for DNA extractions; while fresh leaves were collected from each individual on site and photographed on top of gridded paper for measurements.

nextRAD sequencing

In the nextRAD dataset, the two highest and lowest elevation localities were previously used in a demographic study (Filatov et al., 2016), while the remaining 14 localities are new additions to the dataset. Genomic DNA was extracted from dried leaves using a modified CTAB protocol (Doyle & Doyle, 1987) and purified with QIAGEN DNeasy mini-spin columns. DNA was then sent to SNPsaurus (Oregon, USA), who prepared nextRAD sequencing libraries and carried out 150b single-end Illumina sequencing. This approach is similar to RAD-seq, but uses degenerate primers instead of restriction enzymes.

Analyses of raw reads, genetic diversity and structure in nextRAD dataset

Raw reads from nextRAD sequencing were processed using *STACKS v1.34* (Catchen, Amores, Hohenlohe, Cresko, & Postlethwait, 2011). The *process_radtags* function was used to remove any reads that contained uncalled bases and other low-quality reads. The *denovo_map.pl* script was then used to create a *de novo* catalogue of loci and genotype reads. A minimum stack depth (option -m) of 15, maximum number of mismatches between loci of the same individual (option -M) of two, and maximum number of mismatches between loci in the catalogue (option -n) of two were allowed in making the *de novo* catalogue. The *populations* function was used to call SNPs from the samples, calculate genetic diversity statistics (number of private alleles, percentage of polymorphic loci, observed heterozygosity, expected heterozygosity, nucleotide diversity, inbreeding coefficient, and pairwise F_{ST}), and create genotype input files for further analyses using other software packages. SNPs with 50% or less missing data were retained for subsequent analyses. Isolation by distance was assessed using pairwise genetic distance [$F_{ST}/(1-F_{ST})$] and difference in elevation or geographic distance between locality pairs, with Mantel test, all carried out in *IBD v1.52* (Bohonak, 2002). Analysis

of molecular variance (AMOVA), using only localities involved in demographic modelling, was carried out to test that polymorphism is mostly within species or hybrid groups instead of among individual localities (see demographic modelling section below for details on grouping). To assess the genetic clustering within the dataset, we carried out a principal component analysis (PCA) with the R package *ade4* (Bougeard, 2018; Chessel, Dufour, & Thioulouse, 2004; Dray, Dufour, & Chessel, 2007; Dray & Dufour, 2007) and *factoextra* (Alboukadel & Fabian, 2017). Missing data in PCA were replaced with mean allele frequencies. We also used *STRUCTURE* (Pritchard, Stephens, & Donnelly, 2000) to analyse the clustering of samples. In this analysis, the admixture model was used and the data was run for K = 2 to 18, with 10 iterations for each K. 200,000 generations of burn-in was performed, with 100,000 generations retained. The value for K was then determined using the ad hoc statistic *ΔK* (Evanno, Regnaut, & Goudet, 2005) calculated with *Structure Harvester v0.6.94* (Earl & vonHoldt, 2012).

Demographic modelling using nextRAD data

To explore the demographic history of the two *Senecio* species and their hybrids and visualise the two-dimensional site frequency spectra (2D-SFS), we investigated 14 demographic models (Fig. S2) using Poisson random field-based demography inference framework implemented in the *dadi* package (Gutenkunst, Hernandez, Williamson, & Bustamante, 2009). For this analysis, localities were pooled to represent each of the typical species localities and hybrid localities at the top and bottom of the hybrid zone (inferred from *STRUCTURE* plot): localities 1 to 3 (585 – 910 m) were pooled to represent typical *S. chrysanthemifolius* (C); localities 7 to 9 (1,310 – 1,515 m) were pooled to represent low-elevation hybrids (LH); localities 12 to 14

198 (1,880 – 2,090 m) were pooled to represent high-elevation hybrids (HH); localities 16 to 18
199 (2,386 – 2,645 m) were pooled to represent typical *S. aethnensis* (A). This pooling strategy was
200 necessary to increase the number of samples in each group. To avoid artificially inflating gene
201 flow between groups through pooling localities, AMOVA was carried out to test that
202 polymorphism is mostly within these groupings instead of among individual localities.
203 Moreover, a test run using only one locality of each typical species (locality 1 and 18) were
204 consistent with those from pooled localities. Since no outgroup data was available, folded site
205 frequency spectra (SFS) were generated for each group using the python script easySFS.py
206 (accessed from https://github.com/isaacovercast/easySFS). Following recommendations in
207 the *dadi* manual, each group's sample size was projected down to 10 to 14 alleles (i.e. SNPs
208 with less than these numbers of alleles scored will be removed, and those with more were
209 subsampled to these numbers) to deal with missing data across individuals. SFS of the species
210 pair was first analysed under 14 models of isolation with migration and secondary contact (Fig.
211 S2), which were published previously (Tine et al., 2014; Filatov et al., 2016; Nevado, Contreras-
212 Ortiz, Hughes, & Filatov, 2018) or modified from them. These models vary in complexity (see
213 detailed flow chart in Fig. S2), with the simplest one (*split*) having no population size change
214 and no migration between populations since splitting; to more complex models that allow
215 migration rate in one direction only (e.g. *IM1*, *IM2*), same migration rate for both directions
216 (e.g. *split_mig*, *IM2M_1*), different migration rates in each direction (e.g. *SC*, *IM*, *IMpre*),
217 different migration rates at different times (e.g. *SplitExpMig*, *eSplitExpMig*) or at different
218 parts of genome (e.g. *IM2M*) and population size fluctuations (e.g. *eSplitExpMig*, *IM*, *IMpre*,
219 *IM2M*). Several models are used in this study to test conditions that were not explored before,
220 such as unidirectional gene flow (*IM1*, *IM2*), heterogeneous gene flow (*IM2M*), and a

secondary contact scenario with population size change (*eSC*, *SC_IM2M*). Since the models *IM2M* (heterogeneous gene flow since divergence) and *SC_IM2M* (period of no gene flow followed by heterogeneous gene flow after secondary contact) both have high likelihoods, a more complex model comprising features of both, *IM2M_AL_SC*, was included. This model assumes speciation with heterogeneous gene flow, followed by a period of no gene flow, then secondary contact with heterogeneous gene flow. For all models, 10 runs were performed initially for each data group using a wide parameter range (0 – 5 for time parameters, 0 – 10 for migration parameters, 0 – 100 for size parameters). A further set of 30 runs were then performed using narrower parameter ranges around the optimal values identified in the initial runs.

Since not all the models are nested, the best-fitting model was selected based on Akaike Information Criterion (AIC). The best-fitting model was chosen based on the lowest AIC score. Robustness of parameter estimates of the two best-fitting models was evaluated with 100 bootstrap runs, with the confidence intervals calculated as M ± 1.96X (where M is the likelihood parameter estimate and X is the standard deviation from Godambe Information Matrix (GIM) across replicates). Likelihood ratio tests were performed for nested models to assess which features of models were important in the demographic history of *Senecio* on Mount Etna (refer to Fig. S2 for visualization of models). In particular, *split_mig* and *split* were used to test whether migration has been important; *IM* and *IM1* or *IM2* were used to test whether migration in only one direction would better fit the data; *IM* and *IMpre* were used to test whether there was population size change before the split. *IM2M_1* and *IM2M* were used to test whether having two classes of migration rates provided significantly better fit.

After ranking the demographic models for the pair of pure species, the best model (*IM2M*) and another simpler isolation with migration model (*IM*) were fitted to data from five other comparisons involving pure species and hybrids: high- and low-elevation hybrids (HH/LH), *S. chrysanthemifolius* and low-elevation hybrids (C/LH), *S. chrysanthemifolius* and high-elevation hybrids (C/HH), *S. aethnensis* and low-elevation hybrids (A/LH) and *S. aethnensis* and high-elevation hybrids (A/HH). This is to determine finer scale demographic patterns between species and hybrid localities at different elevations and to compare gene flow in each direction over various spatial separation. These two models have the same type of migration parameters (heterogeneous gene flow or two unidirectional migration) as *SC_IM2M* (the other highly likely model) and *eSC*; they are run since they have fewer parameters than the latter two while yielding the same type of migration data.

Measurement of leaf phenotype

Leaf dissection is the most morphologically distinct character between *S. aethnensis* and *S. chrysanthemifolius*, which have undissected and highly dissected leaves respectively. Hybrids show gradual changes in leaf dissection along the elevation gradient, suggesting that this trait is under divergent selection. To quantify the differences in leaf dissection between the typical species and their hybrids, leaf area to perimeter ratio was used as a proxy for degree of dissection (same trait used in Brennan et al., 2009; 2016). Leaf area to perimeter ratio was calculated from leaf photographs taken at the time of collection. Four to 10 fresh leaves from each individual were collected to control for within individual variability in leaf size. They were photographed on top of gridded paper for measurements. Leaf areas and perimeters were measured using the software ImageJ (Schneider, Rasband, & Eliceiri, 2012). Leaf area to

perimeter ratio was then calculated for each leaf and averaged across leaves for each individual.

Identification of outlier loci in the nextRAD dataset

Fixation index F_{ST} was calculated for each SNP across all samples using *Arlequin* (Excoffier, Laval, & Schneider, 2005), and P values were adjusted for false discovery rate (Benjamini–Hochberg procedure). Negative F_{ST} was treated as zero. Another Bayesian-based outlier scan was carried out using *BayeScan* (Foll & Gaggiotti, 2008) to estimate the probability of a SNP being under selection. This analysis was carried out using default settings: 20 pilots runs of 5,000 iterations, followed by 50,000 burn-in iterations and 5,000 iterations using a thinning interval of 10. Prior odds was set to 10,000. SNPs were treated as outliers if they were significant in both analyses – markers with adjusted P value smaller than 0.05 in Arlequin and $\log_{10}$PO larger than 1 (which indicates selection is 10 times more likely than neutral differentiation at the SNP) in *BayeScan*.

To test if the SNPs are part of or in proximity to any functional genes, a blast search of the loci containing the outlier SNPs was first carried out against genomic scaffolds of *S. squalidus* (unpublished; *S. squalidus* is the hybrid species between *S. aethnensis* and *S. chrysanthemifolius* that originated *ex situ* in the UK). Only non-duplicated matches with at least 95% base pair and 90% identity matched were retained. Sequences within 10 kb from the markers were then blasted against the non-redundant protein sequences database of NCBI. Gene Ontology (GO) terms of top blast hit genes were identified using UniProt (https://www.uniprot.org/).

289 **Cline fitting**

290 Maximum likelihood fitting of clines was done to leaf dissection means or mean allele
291 frequency along the elevational gradient for the leaf area to perimeter ratio, and each of the
292 76 outlier markers. Elevation is used instead of geographic distance because 1) genetic
293 distance has a stronger correlation with difference in elevation than geographic distance (Fig.
294 3); 2) environmental or ecological selective pressures likely change with elevation but not
295 geographic distance; and 3) it allows direct comparison of cline centre and widths at particular
296 elevations in different studies in the system, whereas use of geographic distance would cause
297 confusion as different transects might start and end at different locations. Cline fitting was
298 carried out using the R package *HZAR* (Derryberry, Derryberry, Maley, & Brumfield, 2014).
299 Average leaf area to perimeter ratio of each locality was calculated from the values obtained
300 from ImageJ; input allele frequencies of the nextRAD markers were obtained using *STACKS*.
301 All clines were fitted with three maximum-likelihood models: model I: p_{min}/p_{max} set to
302 observed values without fitting exponential decay curves; model II: p_{min}/p_{max} estimated
303 without fitting any decay curves; and model III: p_{min}/p_{max} estimated with decay curves at both
304 ends fitted (p_{min} and p_{max} denote the lowest and highest average allele frequency in a locality
305 detected for a marker, respectively). The model with the highest likelihood based on AIC
306 scores was chosen for each marker. Cline centre, cline width, minimum and maximum allele
307 frequency observed in each cline, and their two log likelihood (2InL) support limits, were
308 obtained using the same R package. From these measures, maximum change in allele
309 frequency for each marker (Δp) and cline slope (Δp/width) were calculated.

310 An 'average' cline for molecular data was fitted using *STRUCTURE* ancestry scores for
311 tests in cline coincidence (centre) and concordance (width); coincident or concordant clines

312 could mean similar environmental gradient was underlying them. Centres or width of all
313 outlier clines and leaf dissection cline were re-fitted and fixed to those of the *STRUCTURE* cline.
314 The decrease in 2InL after fixing centre or width of each cline were tested using likelihood
315 ratio tests, Bonferroni corrected for multiple tests. Clines were regarded as displaced or
316 discordant with the *STRUCTURE* cline if the decrease in 2InL was significant. Likelihood profiles
317 for selected markers covering the observed range of cline centres and widths were also
318 created (following Phillips, Baird, & Moritz, 2004).
319
320 **Strength of selection**
321 A modified R script (original script provided by van Riemsdijk, Butlin, Wielstra, & Arntzen, 2019)
322 was used to estimate the linkage disequilibrium, dispersal rate, and strength of selection in
323 the hybrid zone. The average dispersal distance per generation (σ) was obtained by $\sqrt{(rDw^2)}$,
324 where r is recombination rate, D is linkage disequilibrium at hybrid zone centre, w is mean
325 cline width of markers used; effective selection against hybrids (s) was obtained by $4\sigma^2/w^2$
326 (Barton & Hewitt, 1985; Szymura & Barton, 1986; 1991; Barton & Gale, 1993). Since
327 recombination rate in the species is not known, a range of 0.1 to 0.5 was used. Forty markers
328 with coincident and concordant clines were used in the estimation of selection (the biggest
329 group of coincident and concordant clines in the dataset). These markers include the 33
330 markers in the elevational range of 1,900 – 2,000 m and with width around 1,200 m (as shown
331 in Fig. 5) and those that are coincident and concordant with them (tested with LRT, using the
332 average centre and width of the group of markers at 1,900 – 2,000 m). Mean and 95%
333 confidence intervals (CI) for linkage disequilibrium and effective selection were calculated
334 with 100 iterations of bootstrapping with replacement.

335

336 **Effect of selection on wider genomic regions**

337 To test whether the signal of selection in the outlier markers (with annotated adjacent genes)
338 was detectable in a wide genomic region, non-outlier SNPs (contained in loci that did not show
339 duplication in blast searches, with 95% base pair and 90% identity matched with genomic
340 scaffolds) closest to the outlier SNPs on the same genomic scaffold were identified and their
341 F_{ST} values were compared to the outlier SNPs.

342

343 ## Results

344 To analyse genetic diversity and divergence among *Senecio* on Mount Etna, we conducted
345 'nextRAD' sequencing for a sample of 192 individuals from 18 localities across an elevational
346 gradient on Mount Etna (Figure 1d). In total, we generated 4.79 x 10^8 sequence reads that
347 were mapped across 513,036 loci identified by *STACKS* (Catchen et al., 2011). Most of these
348 loci (413,124) were invariable, while 99,427 loci contained at least one SNP. Out of these loci,
349 1,769 SNPs with less than 50% missing data were used for analyses.

350

351 **Genetic diversity and structure of localities inferred from nextRAD dataset**

352 Various genetic diversity indices showed substantial variation (Table S1, Fig. S1). In
353 general, *S. chrysanthemifolius* and low-elevation hybrid localities showed higher diversity than
354 *S. aethnensis* and high-elevation hybrid sites. *S. chrysanthemifolius* and low-elevation
355 localities showed generally a higher number of private alleles, a higher percentage of
356 polymorphic loci, higher nucleotide diversity, a lower inbreeding coefficient (F_{IS}), higher
357 observed heterozygosity and lower observed homozygosity (Table S1, Fig. S1). Pairwise F_{ST}

increased with difference in elevation and geographic distance between localities (Fig. 3, Table S2).

After excluding SNPs with more than 50% missing data, 1,769 SNPs were retained for subsequent analyses. In the isolation by distance analysis, genetic distance had a stronger correlation with difference in elevation (Mantel test for genetic distance $F_{ST}/(1-F_{ST})$: $r = 0.79$, $P < 0.001$ in Fig. 3; pairwise F_{ST} matrix in Table S2) than geographic distance between locality pairs ($r = 0.63$, $p < 0.001$). Analysis of molecular variance (AMOVA) showed that most genetic variation is found among species or hybrid groupings (37.05%) and among individuals (58.98%) (Table 2). *STRUCTURE* and subsequent analyses revealed the optimal number of clusters (K) is two (Fig. 1c; the same dataset but with the 76 SNP outliers excluded showed the same results thus results from the 1769-SNP dataset was used in all subsequent analyses). Most individuals at the two ends of the elevational gradient clustered into two distinct groups, each presumably representing one typical ('pure') species; admixed individuals were found at intermediate elevations, with a varying proportion of each cluster. There is a small amount of admixture detected in very high-elevation *S. aethnensis* samples, while very low-elevation *S. chrysanthemifolius* does not show any admixture. Principal components analysis (PCA; Fig 2) does not show conspicuous clustering of populations, but a gradual transition between high and low elevation samples. PC 1 shows high-elevation samples being more evenly distributed across the principal component while low-elevation ones are more clustered with several outliers in high-elevation samples' space. PC 2 shows rough clustering of each of the pure species and hybrids.

Cline in leaf dissection

381 The change in leaf area to perimeter ratio shows a clinal pattern (Fig. 4). The cline showed a
382 rapid change in leaf area to perimeter ratio around the elevation of 1,900 m, with the cline
383 centre estimated at 1,910 m (2InL = 1,882 – 1,935 m), and the cline width of 127 m (2InL = 51
384 – 196 m).
385
386 **Identification of outlier nextRAD markers and analysis of their clines**
387 To identify highly differentiated markers, we used *Arlequin* and *Bayescan.* The F_{ST} values,
388 calculated for each SNP using *Arlequin*, ranged from 0 to 0.8587 (mean F_{ST} = 0.0854). 183 SNPs
389 were identified as outliers based on F_{ST} values (Fig. S3). *BayeScan* identified 89 SNPs with high
390 F_{ST} and $\log_{10}PO > 1$ (Fig S4), indicating they are likely to be under divergent selection.
391 A total of 76 SNPs were identified as outliers as they were significant in both outlier
392 analyses. Distribution of these markers' maximum change in allele frequency, cline centre,
393 cline width and cline slope are shown in Table S5 and Fig. S5. Cline centre positions showed a
394 peak at 1,900 – 2,000 m (Fig. S5b). Cline width showed some variability (Fig. S5c), while cline
395 slope (< 0.01) were small for most markers (Fig. S5d). Cline width did not show correlation
396 with cline centre position (Fig. S5e). However, clines centred at around 1,900 m showed
397 especially steep slopes (Fig. S5f). The *STRUCTURE* cline, which acts as the 'average' cline for
398 tests of coincidence and concordance, has a centre and width of 1852 m and 866 m
399 respectively. Among the 76 outlier clines, 51 and 40 were coincident and concordant with the
400 *STRUCTURE* cline respectively; while 18 were both coincident and concordant with the
401 *STRUCTURE* cline (Table S4). These indicate that clines show significantly variable coincidence
402 and concordance. In general, clines with more similar cline centres are more likely to be
403 coincident. The leaf dissection cline is coincident but discordant with the *STRUCTURE* cline.

404

405 **Potential association between outlier markers and functional genes**

406 Blast searches of outlier markers against scaffolds of unpublished *Senecio squalidus* draft
407 genome and the non-redundant protein sequences database of NCBI led to the identification
408 of 17 genes located within or in proximity (within 10 kb) of the markers (see Fig. 4 for clines;
409 Table S3 for position of markers on scaffolds or distance from functional genes) associated
410 with different functions. Some outlier genes' functions have no apparent association with
411 adaptation to contrasting environments on Mount Etna; while other genes identified are
412 involved in photosynthesis, defence response, photoperiodism, flowering, metal ion binding,
413 and response to UV, which could underlie environmental or ecological adaptation, or
414 reproductive isolation. The details about these genes, including blast results, outlier analyses
415 results, cline statistics, gene annotations, and information about the markers nearest to these
416 genes are summarised in Table S3.

417

418 **Strength of selection**

419 Population linkage disequilibrium of the 40-marker dataset with coincident and concordant
420 clines (Table S5) is elevated at the hybrid zone centre at around 1,900 – 2,000 m in elevation
421 (Fig. S7). Linkage disequilibrium estimated for the cline centre is 0.3915 (95% CI = 0.3681 –
422 0.4119). The dispersal rate was estimated to be 0.56 – 1.27 km/gen (corresponding to 144 –
423 323 m in elevation) and the corresponding average effective selection is 0.1565 (95% CI =
424 0.1472 - 0.1648) and 0.7831 (95% CI = 0.7521 - 0.8144), assuming recombination rate of 0.1
425 and 0.5 respectively.

426

How wide are the genomic regions affected by divergent selection?

Identifying non-outlier SNPs (noSNPs) that are closest to the 17 outliers (oSNPs) through blasting of adjacent regions (same criteria as identifying genomics scaffolds for outliers), it was revealed that the distance between the noSNPs and oSNPs (that fall within the same scaffold) range from around 50 kb to 1.3 mb, with F_{ST} for noSNPs ranging from 0 to 0.19. For some genomic regions, noSNPs with F_{ST} less than 0.047 are located as close as 51 kb to oSNPs (e.g. marker 10586 in Table S3); while in other regions, the distance was much longer and the noSNP's F_{ST} was not as low (e.g. 400 kb and F_{ST} = 0.20 for marker 185 in Table S3). This indicates that the signal of selection in the genomes of Etnean *Senecio* species may be very localised. Further work has to be done to study the selection patterns (and evaluate the effect of missing data) in detail.

Demographic history of *Senecio* on Mount Etna

We first focused on the analysis of demographic history between the pure species, as done in our previous work (Filatov et al., 2016). That previous work was focusing on overall species demography and did not consider the possibility that different parts of the genome may have different rates of interspecific gene flow due to selection preventing introgression of some genomic regions. To take the possibility of heterogeneous gene flow across the genome into account, we allowed an *IM* model to have two bi-directional migration parameters, M_A and M_B (model *IM2M*, Figure 6a). The *IM2M* model fits data significantly better than the models without heterogeneous migration (AIC score = 399.04; Table 3, Fig. 6a). Another model, *SC_IM2M*, was almost as likely (AIC score = 399.14; Table 3, Fig 6b). Both models involve heterogeneous gene flow, with the higher migration rates being 4.38 and 4.96 times larger

than the other lower ones for the models *IM2M* and *SC_IM2M* respectively. Likelihood ratio tests (LRT) were carried out for five groups of nested models. The LRT between *IMpre* and *IM* models was not significant (p-value = 0.57), indicating that allowing for an ancestral population size change prior to species split (in model *IMpre*) does not significantly improve the fit to data. LRT for other four model comparisons were significant. In particular, allowing for migration dramatically improves the fit to data compared to the nested model without migration (*split_mig* versus *split*, p-value = 1.76×10^{-30}). Allowing migration in both directions significantly improves the fit to data compared to unidirectional migration (*IM* versus *IM1* or *IM2*, p-value = 5.55×10^{-13} and 3.74×10^{-16} respectively). Having two separate classes of bi-directional migration significantly improves model fit compared to only one class of migration (*IM2M* versus *IM2M_1*, p-value = 0.0066). These results indicate that the genomes are experiencing gene flow in both directions and that gene flow is heterogeneous (i.e. a fraction of the genome is exchanging alleles significantly less than the rest of the genome). Although the models assuming heterogeneous gene flow did not test for symmetry of gene flow in each class, results from models with separate parameters for different directions of migration (*IM*, *IMpre*, *SC*, *eSC*; see Table 3) suggest that gene flow in the same class is slightly asymmetric. Migration rate from *S. chrysanthemifolius* to *S. aethnensis* is 1.24 to 1.70 times higher than from *S. chrysanthemifolius* to *S. aethnensis*.

The best fitting model (*IM2M*) was also fitted to data from other pairwise comparisons of species and hybrid groups to investigate different demographic parameters at a finer scale. Another isolation with migration model, *IM*, was also run to assess the relative amount of gene flow in each direction in different comparisons (see parameters in Table 3). All groups show smaller current population sizes compared to their ancestral sizes. In all species/hybrid

comparisons (C/LH, C/HH, A/LH, A/HH, where C = *S. chrysanthemifolius*, A = *S. aethnensis*, LH – low-elevation hybrids and HH = high-elevation hybrids) under the model *IM2M*, one class of migration is always at least twice (2.3 to 8.5 times) larger than the other one. Migration is also higher between localities that are closer to each other (C/LH and A/HH) than those further apart (C/HH and A/LH). Under the *IM* model, the migration rate from the pure species to hybrids (M_{21}) is 1.6 to 3 times larger than that in the opposite direction (M_{12}).

In the high- and low-elevation hybrids comparison (HH/LH), the two classes of migration rate are both high under the model *IM2M* (3.61 and 2.26) and *IM* (3.72 and 3.04), likely indicating most of their genomes share genes more freely (instead of having regions with restricted gene flow).

Discussion

Hybrid zones are a powerful tool to study the dynamics of phenotypic and genotypic divergence between closely related species; also, recently diverged species offer great opportunities to catch 'speciation in action' by studying the patterns of gene flow and genomic heterogeneity in taxa subject to divergent selection (Via, 2009). *S. aethnensis* and *S. chrysanthemifolius* on Mount Etna are characterised by a hybrid zone and recent divergence less than 200,000 years ago. Using genome-wide SNPs in samples comprising both species and their hybrids, we investigated demographic features, patterns of gene flow and selection in this system, and factors that are likely contributing to maintenance of divergence in the face of on-going gene flow between the two species.

Demographic history of speciation in Etnean *Senecio*

Various demographic models implemented in *dadi* (see Fig. S2 for visualisation of models) were used to reconstruct the most likely speciation scenario and demographic features in the divergence of *S. aethnensis* and *S. chrysanthemifolius* on Mount Etna.

Our analysis revealed that the *IM2M* model fits the data best. This model has not been considered in previous studies in *Senecio*, but some of the parameter estimates are similar to that obtained previously. In particular, migration between the two pure species inferred here is similar to the estimate from the most likely model in Filatov et al. (2016), which is less than one migrant per generation on average (average between M_A and M_B; number of migrants per generation is higher in other geographically closer comparisons in the current study). Given models with (*SC_IM2M*) and without (*IM2M*) secondary contact both have high relative likelihoods, there is little power in the data to distinguish between these demographic scenarios; it may also be seen as a lack of evidence for the secondary contact scenario as the more complex *SC_IM2M* model did not significantly improve fit to data (consistent with Filatov et al.; 2016). What is common between both models is that they both involve heterogeneous gene flow. This indicates that a fraction of the genome introgresses considerably slower compared to the rest of the genome, possibly due to intrinsic or extrinsic selection against introgressed alleles in these regions. Many studies have demonstrated heterogeneous divergence in different genomes and that divergent selection has a crucial role in genomic heterogeneity (reviewed in Nosil, Funk, & Ortiz-Rrientos, 2009).

Another interesting point to note is that gene flow is highly asymmetric, as revealed by four models for the pure species comparison and *IM* analyses of other pure species/ hybrid comparisons. Gene flow from *S. chrysanthemifolius* to *S. aethnensis* is 1.24 to 1.70 times higher than from *S. aethnensis* to *S. chrysanthemifolius*; while gene flow is always (1.6 to 3

519 times) greater from pure species to hybrids, compared to gene flow from hybrids to pure
520 species. This low rate of introgression from hybrid to pure species could be caused by various
521 reasons, such as lower reproductive fitness in hybrids, and low rate of backcrossing. The
522 directionality of gene flow helps to explain the apparent contradiction between plentiful
523 evidence of hybridisation at intermediate elevations and relatively modest estimates of gene
524 flow between the pure species at the two extremes of the elevational cline.
525
526 **Variable coincidence and concordance among phenotypic and genotypic clines**
527 We fitted clines for leaf dissection and genetic markers using the same individuals. Likelihood
528 ratio tests revealed that clines have significantly variable coincidence and concordance.
529 Although clines studied here have variable coincidence, they are all centred in the putative
530 hybrid zone (1,200 – 2,000 m in elevation), with only a few exceptions that are centred above
531 2000 m (this corresponds to the observation in the *STRUCTURE* analysis where there is a little
532 admixture in high-elevation *S. aethnensis*). These environmental and ecological factors likely
533 vary in different ways with regard to elevations within the hybrid zone. Other studies, such as
534 those on the marine snails *Littorina saxatilis*, have also suggested displaced clines among
535 different environmental transitions that would lead to selection acting on different loci
536 independently (e.g. Hollander, Galindo, & Butlin, 2015). Like the current study, many studies
537 on these snails have also identified genomic regions under divergent selection and associated
538 with adaptive phenotypic traits (Hollander et al., 2015; Pennec et al., 2017; Westram et al.,
539 2014).
540 Analysing allozymes, simple sequence repeats (SSR) and various groups of phenotypic
541 measurements, Brennan et al. (2009) found highly coincident and concordant clines among

all of them, in which they are centred at 6.67 – 7.82 km (corresponding to elevations somewhere between 1,515 – 1,928 m) with widths of 1.49 – 3.7 km. In particular, they found the leaf structure cline to be centred at 6.67 (6.25 – 6.97) km with width of 1.49 (0.06 – 2.39) km. These support limits translate into cline centre within the elevational range of 1,515 – 1,795 m and width of more than 400 m in elevation. Brennan et al. (2009)'s leaf structure cline does not seem to be coincident with the leaf dissection cline in this study, while the cline width in this study is well within the range reported by Brennan et al. (2009) [in the current study, cline centre = 1,910 (1,882 – 1,935) m; width = 127 (51 – 196 m)]. The discrepancy could be due to: 1) more than one leaf traits were combined in the leaf structure cline in Brennan et al. (2009). Individual leaf trait clines might have centres and widths different from leaf dissection; 2) samples in Brennan et al. (2009) were collected from a few areas located on different sides of Mount Etna, while samples in this study were collected along a more or less straight transect on the southern side of the mountain. Hence, results in the two studies should be compared with caution.

Strong selection against hybrids on Mount Etna

Effective selection against hybrids inferred in this study (0.16 – 0.78 assuming recombination between the markers is r = 0.1 – 0.5) is much higher than that in Brennan et al. (2009) (0.02 – 0.11 for r = 0.1 – 0.5 respectively) for the same species. Dispersal rate inferred in this study (0.56 – 1.27 km/gen for r = 0.1 – 0.5) is also greater than that in Brennan et al. (2009) (0.17 – 0.38 km/gen for r = 0.1 – 0.5). Both studies used only coincident and concordant clines in estimating selection, thus the difference could be related to the type of markers used (allozymes and microsatellites in Brennan et al. (2009); SNPs in the current study). For instance,

565 microsatellites have multiple alleles, hence higher heterozygosities and mutation rate than
566 SNPs (Mueller, 2004); these properties could lead to different estimates of linkage
567 disequilibrium and subsequent estimates. In our analysis, linkage disequilibrium is elevated at
568 the hybrid zone centre, which is expected for a hybrid zone experiencing strong selection.
569 However, linkage disequilibrium in the high-elevation localities for *S. aethnensis* is also quite
570 high. This could be caused by an influx of alleles from *S. chrysanthemifolius*, as revealed by the
571 presence of admixed individuals in high-elevation localities in the *STRUCTURE* analysis, and
572 asymmetric migration in demographic modelling.

573 Estimates of selection and dispersal from a recombination rate of 0.5 (the higher
574 values) are probably closer to reality as it is unlikely that all markers used are tightly clustered.
575 Our selection estimate from this recombination rate corresponds to a 78% drop in fitness in
576 hybrids in the centre of hybrid zone, which indicates that the *Senecio* cline is maintained by
577 fairly strong selection. This is one of the highest estimates reported (Table 1). Previous studies
578 on salamanders (Alexandrino et al., 2005) and skinks (Phillips et al., 2004) have reported
579 values similar to the current study, yet they calculated selection using $s = 8\sigma^2/w^2$ while our
580 study used $s^* = 4\sigma^2/w^2$ (Table 1; $s^* = 4\sigma^2/w^2$ measures the difference in mean fitness between
581 centre and edge of hybrid zone, and measuring this difference in mean fitness makes selection
582 estimates comparable between different forms of selection; whereas $s = 8\sigma^2/w^2$ assumes half
583 of the individuals are heterozygotes at the hybrid zone centre, where $s = 2s^*$). In other words,
584 the estimate in the current study (0.78) is at least two, and up to more than 200, times larger
585 than that in other recent studies presented in Table 1 after accounting for the fold differences
586 in the formulae used. It is worth noting that Brennan et al. (2009) also calculated effective

587 selection in Etnean *Senecio* with $8\sigma^2/w^2$, though this does not account for the difference
588 between the estimates in their and the current studies either.

589 The inferred dispersal (0.56 – 1.27 km/gen) is rather small, compared to what one
590 would expected for wind-dispersed herbaceous plants. This, together with strong selection
591 against hybrids and demographic modelling showing around one migrant per generation,
592 collectively indicate that gene flow is restricted, likely due to divergent selection. Selection
593 against hybrids has only been shown to manifest as hybrid breakdown in F_2 plants in two
594 crosses in two studies (Brennan et al., 2014; Chapman et al., 2016), thus larger-scale studies
595 are required to further investigate the effect on hybrid establishment and fitness. Multifarious
596 selection is evident in this system, as clines of many outlier markers are relatively wide (hence
597 selection at many individual traits is unlikely to be strong) while a few show rather narrow
598 clines with widths under 100 m; and only a small proportion of clines is coincident and
599 concordant. The strong selection against hybrids and occurrence of multifarious selection
600 likely facilitates local adaptation in the two species and their divergence. Future work that
601 analyses how potential environmental or ecological selective forces (for example, whether
602 they change gradually or abruptly along the gradient and how different their effects are) had
603 shaped the system would be particularly fascinating for this young but complex system.

604

605 **Intrinsic and extrinsic causes in the divergence of Etnean *Senecio***

606 Regardless of the speciation scenario at the start of divergence, Etnean *Senecio* has
607 experienced heterogeneous gene flow. One question that arises from this is whether selective
608 sweeps [leading to (near-) fixation of SNPs in populations of pure species] or barriers to gene
609 flow (selection in the hybrid zone in this case) cause divergence in this differentiated portion

of genome (Tavares et al., 2018). Both of these would show signatures of divergent selection, and disentangling between the two would require higher-resolution genomic data. It would also be interesting to quantify the regions and extent of frequent or rare migration in the genome in future studies.

Research on intrinsic incompatibilities is often disconnected from studies of extrinsic selection, making integrating different components of reproductive isolation challenging (Seehausen et al., 2014). With both intrinsic incompatibility and multifarious divergent selection, the Etnean *Senecio* allows one to combine both directions of research to study the interplay between intrinsic and extrinsic processes. This adds to the limited literature in other systems which also have evidence for both, including in killfish, *Lucania*, where there is extrinsic isolation caused by salinity and intrinsic incompatibilities (Fuller, 2008); and in the copepod *Tigriopus californicus*, where interpopulation hybrids show adaptation to different thermal conditions and intrinsic incompatibilities (Ellison & Burton, 2006, 2008; Willett, 2010). However, unlike these systems, the Etnean *Senecio* is parapatric and multifarious selection might be crucial in creating strong enough reproductive isolation to allow the accumulation and maintenance of genetic divergence in the system (Seehausen et al., 2014).

Maintenance of divergence despite gene flow

It is intriguing how the pair of sister *Senecio* species maintain their divergence while hybridising in the relatively small area of Mount Etna. Yet, this phenomenon is not uncommon - Quercus (oaks) and *Populus* (poplars) are well-studied groups with a 'porous' species boundary. Studies in these two groups have shown that their species identities are maintained by an array of mechanisms, some of which have been presented or observed in the Etnean

Senecio. These include, in oaks, divergent selection (Ortego, Gugger, & Sork, 2017; Scotti-Saintagne et al., 2004), and asynchrony in flowering leading to assortative mating (Gailing & Curtu, 2014); in poplars, intrinsic incompatibility (Christe et al., 2017; Roe et al., 2014), and selection against hybrids (Christe et al., 2016). It is plausible that a combination of divergent selection, strong cumulative selection against hybrids and difference in phenology (such as flowering times) helps to reinforce the reproductive isolation in the system. Given the prevalence of hybridisation between closely-related plant species across different families, these systems point to the possibility that more unstudied plant groups and species complexes might have extensive hybridisation while maintaining their respective species boundaries or divergence at the sub-species levels. Studying these groups would greatly benefit the field of plant hybridisation, speciation with gene flow, and study of the role of gene flow, selection and introgression in adaptation and speciation.

Conclusion

In this study, we have shown that only a small proportion of differentiated loci (76 out of 1,769 studied) and strong cumulative multifarious selection at a handful of genes are likely involved in keeping the two Etnean *Senecio* species distinct. Although the exact mechanism of speciation in this system is far from clear, this study has added to the body of evidence that both intrinsic and extrinsic processes have roles in speciation and maintenance of divergence in the face of gene flow (Ellison & Burton, 2006, 2008; Fuller, 2008; Willett, 2010). To summarise, we have 1) shown heterogeneous, bidirectional gene flow, and population size changes in the past are characteristics of the speciation of Etnean *Senecio*; 2) discovered promising candidate genes that are potentially linked to local adaptation; 3) inferred the likely

presence of multifarious selective forces of different strengths; and 4) estimated strong selection against hybrids. It is crucial to extend this work by identifying the selective forces underlying divergence and linking them to elevation or ecology, analysing fine-scale genomic patterns that harbour regions of interests, the interplay between intrinsic incompatibilities and extrinsic, multifarious environmental selection in shaping the system, and the potential role of other genetic phenomena (such as genetic hitchhiking and chromosomal rearrangement) in causing divergence.

Acknowledgements

This work was funded by grants to DAF from NERC and BBSRC. We would like to thank Isolde van Riemsdijk (NCB Naturalis) and Prof. Roger Butlin (University of Sheffield and University of Gothenburg) for kindly providing and helping to modify the R script and discussion of the relevant analyses. We are also grateful for Prof. Roger Butlin and anonymous reviewers for providing comments on the manuscript.

References

Alboukadel, K., & Fabian, M. (2017). factoextra: Extract and Visualize the Results of Multivariate Data Analyses.

Alexandrino, J., Baird, S. J., Lawson, L., Macey, R. J., Moritz, C., & Wake, D. B. (2005). Strong selection against hybrids at a hybrid zone in the Ensatina ring species complex and its evolutionary implications. *Evolution*, *59*(6), 1334–1347. doi:10.1554/04-156

Antonovics, J., & Bradshaw, A. D. (1970). Evolution in closely adjacent plant populations VIII. Clinal patterns at a mine boundary. *Heredity*, *25*(3*)*, 349–362. doi:10.1038/hdy.1970.36

Bailey, R. I., Tesaker, M. R., Trier, C. N., & Sætre, G.-P. (2015). Strong selection on male plumage in a hybrid zone between a hybrid bird species and one of its parents. *Journal of Evolutionary Biology*, *28*(6), 1257–1269. doi:10.1111/jeb.12652

Baldassarre, D. T., White, T. A., Karubian, J., & Webster, M. S. (2014). Genomic and morphological analysis of a semipermeable avian hybrid zone suggests asymmetrical introgression of a sexual signal. *Evolution*, *68*(9), 2644–2657. doi:10.1111/evo.12457

Barton, N. H., & Gale, K. S. (1993). Genetic analysis of hybrid zones. In:, pp. 13–45. Oxford University Press.

Barton, N. H., & Hewitt, G. M. (1985). Analysis of Hybrid Zones. *Annual Review of Ecology and Systematics*, *16*(1), 113–148.

Bohonak, A. J. (2002). IBD (Isolation by Distance): A Program for Analyses of Isolation by Distance. *Journal of Heredity*, *93*, 153–154. doi:10.1093/jhered/93.2.153

Bougeard, S., & Dray, S. (2018). Supervised Multiblock Analysis in R with the ade4 Package. *Journal of Statistical Software*, *86*(1). doi:10.18637/jss.v086.i01

Brelsford, A., & Irwin, D. (2009). Incipient Speciation Despite Little Assortative Mating: The Yellow-Rumped Warbler Hybrid Zone. *Evolution*, *63*(12), 3050–3060. doi:10.1111/j.1558-5646.2009.00777.x

Brennan, A. C., Bridle, J. R., Wang, A.-L., Hiscock, S. J., & Abbott, R. J. (2009). Adaptation and selection in the *Senecio* (Asteraceae) hybrid zone on Mount Etna, Sicily. *The New phytologist*, *183*, 702–17. doi:10.1111/j.1469-8137.2009.02944.x

Brennan, A. C., Hiscock, S. J., & Abbott, R. J. (2014). Interspecific crossing and genetic maping reveal intrinsic genomic incompatibility between two *Senecio* species that form a hybrid zone on Mount Etna, Sicily. *Heredity*, *113*, 195-204. doi:10.1038/hdy.2014.14

Brennan, A. C., Hiscock, S. J., & Abbott, R. J. (2016). Genomic architecture of phenotypic divergence between two hybridizing plant species along an elevational gradient. *AoB PLANTS*, *8*, plw022. doi:10.1093/aobpla/plw022

Brennan, A. C., Hiscock, S. J., & Abbott, R. J. (2019). Completing the hybridization triangle: the inheritance of genetic incompatibilities during homoploid hybrid speciation in ragworts (Senecio). *AoB PLANTS*, *11*(1), ply078. doi:10.1093/aobpla/ply078

Carneiro, M., Baird, S., Afonso, S., Ramirez, E., Tarroso, P., Teotónio, H., … Ferrand, N. (2013). Steep clines within a highly permeable genome across a hybrid zone between two subspecies of the European rabbit. *Molecular Ecology*, *22*(9), 2511–2525. doi:10.1111/mec.12272

Catchen, J. M., Amores, A., Hohenlohe, P., Cresko, W., & Postlethwait, J. H. (2011). Stacks: Building and Genotyping Loci De Novo From Short-Read Sequences. *G3: Genes, Genomes, Genetics*, *1*, 171–182. doi:10.1534/g3.111.000240

Chapman, M. A., Forbes, D. G., & Abbott, R. J. (2005). Pollen competition among two species of *Senecio* (Asteraceae) that form a hybrid zone on Mount Etna, Sicily. *American journal of botany*, *92*, 730–735. doi:10.3732/ajb.92.4.730

Chapman, M. A., Hiscock, S. J., & Filatov, D. A. (2013). Genomic Divergence during Speciation Driven by Adaptation to Altitude. *Molecular Biology and Evolution*, *30*, 2553–2567. doi:10.1093/molbev/mst168

Chapman, M. A., Hiscock, S. J., & Filatov, D. A. (2016). The genomic bases of morphological divergence and reproductive isolation driven by ecological speciation in *Senecio* (Asteraceae). *Journal of Evolutionary Biology*, *29*, 98–113. doi:10.1111/jeb.12765

Chessel, D., Dufour, A., & Thioulouse, J. (2004). The ade4 Package - I: One-Table Methods. *R News*, *4*(1), 5–10.

Christe, C., Stölting, K., Bresadola, L. *et al.* (2016). Selection against recombinant hybrids maintains reproductive isolation in hybridizing *Populus* species despite F_1 fertility and recurrent gene flow. *Molecular Ecology*, *25*, 2482–2498. doi.org/10.1111/mec.13587

729 Christe, C., Stölting, K., Paris, M. *et al.* (2017). Adaptive evolution and segregating load
730 contribute to the genomic landscape of divergence in two tree species connected by
731 episodic gene flow. *Molecular Ecology*, *26*, 59–76. doi:10.1111/mec.13765
732 Daroski, H., Feder, J. (2007). Host plant and latitude-related diapause variation in *Rhagoletis*
733 *pomonella*: a test for multifaceted life history adaptation on different stages of diapause
734 development. *Journal of Evolutionary Biology*, *20*, 2101–2112. doi:10.1111/j.1420-
735 9101.2007.01435.x
736 Delmore, K., & Irwin, D. (2014). Hybrid songbirds employ intermediate routes in a migratory
737 divide. *Ecology Letters*, *17*(10), 1211–1218. doi.org/10.1111/ele.12326
738 Derryberry, E. P., Derryberry, G. E., Maley, J. M., & Brumfield, R. T. (2014). hzar: hybrid zone
739 analysis using an R software package. *Molecular Ecology Resources*, *14*, 652–663.
740 doi:10.1111/1755-0998.12209
741 Doyle, J. J., & Doyle, J. (1987). A rapid DNA isolation procedure for small quantities of fresh
742 leaf tissue. *Phytochemisty Bulletin*, *19*, 11–15.
743 Dray, S., Dufour, A., & Chessel, D. (2007). The ade4 Package - II: Two-Table and K-Table
744 Methods. *R News*, *7*(2), 47–52. doi:10.18637/jss.v022
745 Dray, S., & Dufour, A. (2007). The ade4 Package: Implementing the Duality Diagram for
746 Ecologists. *Journal of Statistical Software*, *22*(4), 1–20.
747 Durrett, R., Buttel, L., & Harrison, R. (2000). Spatial models for hybrid zones. *Heredity*, *84*(1),
748 6885660. 6885660. doi:10.1046/j.1365-2540.2000.00566.x
749 Earl, D. A., & vonHoldt, B. M. (2012). STRUCTURE HARVESTER: a website and program for
750 visualizing STRUCTURE output and implementing the Evanno method. *Conservation*
751 *Genetics Resources*, *4*, 359–361. doi:10.1007/s12686-011-9548-7
752 Egea-Serrano, A., Hangartner, S., Laurila, A., Räsänen, K. (2014). Multifarious selection through
753 environmental change: acidity and predator-mediated adaptive divergence in the moor
754 frog (*Rana arvalis*). *Proceedings of the Royal Society B: Biological Sciences*, *281*,
755 20133266. doi:10.1098/rspb.2013.3266
756 Ellison, C. K., Burton, R. S. (2006). Disruption of mitochondrial function in interpopulation
757 hybrids of *Tigriopis californicus*. *Evolution*, *60*, 1382–1391. doi:10.1554/06-210.1
758 Ellison, C. K., Burton, R. S. (2008). Interpopulation hybrid breakdown maps to the
759 mitochondrial genome. *Evolution*, *62*, 631–638. doi:10.1111/j.1558-5646.2007.00305.x
760 Evanno, G., Regnaut, S., & Goudet, J. (2005). Detecting the number of clusters of individuals
761 using the software structure: a simulation study. *Molecular Ecology*, *14*, 2611–2620.
762 doi:10.1111/j.1365-294X.2005.02553.x
763 Excoffier, L., Laval, G., & Schneider, S. (2005). Arlequin (version 3.0): An integrated software
764 package for site genetics data analysis. *Evolutionary Bioinformatics*, *1*,
765 117693430500100003. doi:10.1177/117693430500100003
766 Feder, J. L., Egan, S. P., & Nosil, P. (2012). The genomics of speciation-with-gene-flow. *Trends*
767 *in Genetics*, *28*, 342–350. doi:10.1016/j.tig.2012.03.009
768 Filatov, D. A., Osborne, O. G., & Papadopulos, A. S. T. (2016). Demographic history of
769 speciation in a *Senecio* altitudinal hybrid zone on Mount Etna. *Molecular Ecology*, *25*,
770 2467–2481. doi:10.1111/mec.13618
771 Foll, M., & Gaggiotti, O. (2008). A genome-scan method to identify selected loci appropriate
772 for both dominant and codominant markers: a Bayesian perspective. *Genetics*, *180*,
773 977–93. doi:10.1534/genetics.108.092221

774 Fuller, R. C. (2008). Genetic incompatibilities in killfish and the role of environment. *Evolution*,
775 *62*, 3056–3068. doi:10.1111/j.1558-5646.2008.00518.x
776 Gailing, O., Curtu, A. (2014). Interspecific gene flow and maintenance of species integrity in
777 oaks. *Annals of Forest Research*, *0*, 1–14. doi:10.15287/afr.2014.171
778 Gompert, Z., Lucas, L., Nice, C. et al. (2013). Geographically multifarious phenotypic
779 divergence during speciation. *Ecology and Evolution*, *3*, 595–613. doi:10.1002/ece3.445
780 Gutenkunst, R. N., Hernandez, R. D., Williamson, S. H., & Bustamante, C. D. (2009). Inferring
781 the Joint Demographic History of Multiple Sites from Multidimensional SNP Frequency
782 Data. *PLoS Genetics*, *5*, e1000695. doi:10.1371/journal.pgen.1000695
783 Hollander, J., Galindo, J., & Butlin, R. K. (2015). Selection on outlier loci and their association
784 with adaptive phenotypes in Littorina saxatilis contact zones. *Journal of Evolutionary*
785 *Biology*, *28*(2), 328–337. doi:10.1111/jeb.12564
786 James, J. K., & Abbott, R. J. (2005). Recent, allopatric, homoploid hybrid speciation: the origin
787 of *Senecio squalidus* (Asteraceae) in the British Isles from a hybrid zone on Mount Etna,
788 Sicily. *Evolution*, *59*(12):2533-2547. doi:10.1554/05-306.1
789 Kawakami, T., Butlin, R. K., Adams, M., Paull, D. J., & Cooper, S. J. (2009). Genetic analysis of a
790 chromosomal hybrid zone in the Australian morabine grasshoppers (Vandiemenella,
791 Viatica species group). *Evolution*, *63*(1), 139–152. doi.org/10.1111/j.1558-
792 5646.2008.00526.x
793 Kruuk, L. E., Baird, S. J., Gale, K. S., & Barton, N. H. (1999). A comparison of multilocus clines
794 maintained by environmental adaptation or by selection against hybrids. *Genetics*,
795 *153*(4), 1959–71.
796 Körner, C. (2007). The use of “altitude” in ecological research. *Trends in Ecology & Evolution*,
797 *22*, 569–574. doi:10.1016/j.tree.2007.09.006
798 Macholn, M., Munclinger, P., Šugerkov, M., Dufkov, P., Bmov, B., Božkov, E., … Pilek, J. (2007).
799 Genetic analysis of autosomal and X-linkedmarkers across a mouse hybrid zone.
800 *Evolution*, *61*(4), 746–771. doi.org/10.1111/j.1558-5646.2007.00065.x
801 Mallet, J. (2005). Hybridization as an invasion of the genome. *Trends in Ecology & Evolution*,
802 *20*, 229–37. doi:10.1016/j.tree.2005.02.010
803 Mueller, J. (2004). Linkage disequilibrium for different scales and applications. *Briefings in*
804 *Bioinformatics*, *5*(4), 355–364. doi:10.1093/bib/5.4.355
805 Muir, G., Osborne, O., Sarasa, J., Hiscock, S., & Filatov, D. (2013). Recent ecological selection
806 on regulartory divergence is shaping clinal variation in *Senecio* on Mount Etna. *Evolution*,
807 *67*, 3032–3042. doi:10.1111/evo.12157
808 Nevado, B., Contreras-Ortiz, N., Hughes, C., & Filatov, D. A. (2018). Pleistocene glacial cycles
809 drive isolation, gene flow and speciation in the high-elevation Andes. *New Phytologist*,
810 *219*, 779–793. doi:10.1111/nph.15243
811 Nosil, P., Funk, D. J., & Ortiz-Barrientos, D. (2009). Divergent selection and heterogeneous
812 genomic divergence. *Molecular Ecology*, *18*(3), 375–402. doi:10.1111/j.1365-
813 294X.2008.03946.x
814 Nosil, P., Harmon, L., Seehausen, O. (2009) Ecological explanations for (incomplete) speciation.
815 *Trends in Ecology & Evolution*, *24*, 145–156. doi:10.1016/j.tree.2008.10.011
816 Ortego, J., Gugger, P., Sork, V. (2017). Impacts of human-induced environmental disturbances
817 on hybridization between two ecologically differentiated Californian oak species. *New*
818 *Phytologist*, *213*, 942–955. doi:10.1111/nph.14182

819 Osborne, O., Batstone, T. E., Hiscock, S. J., & Filatov, D. A. (2013). Rapid Speciation with Gene
820 Flow Following the Formation of Mount Etna. *Genome Biology and Evolution*, *5*, 1704–
821 1715. doi:10.1093/gbe/evt127
822 Phillips, B. L., Baird, S. J., Moritz, C. (2004). When vicars meets: a narrow contact zone between
823 morphologically cryptic phylogeographic lineages of the Rainforest Skink, *Carlia*
824 *Rubrigularis*. *Evolution*, *58*, 1536–1548. doi:10.1111/j.0014-3820.2004.tb01734.x
825 Polyakov, A. V., White, T. A., Jones, R. M., Borodin, P. M., & Searle, J. B. (2011). Natural
826 hybridization between extremely divergent chromosomal races of the common shrew
827 (Sorex araneus, Soricidae, Soricomorpha): hybrid zone in Siberia. *Journal of Evolutionary*
828 *Biology*, *24*(7), 1393–1402. doi:10.1111/j.1420-9101.2011.02266.x
829 Pritchard, J., Stephens, M., & Donnelly, P. (2000). Inference of site structure using multilocus
830 genotype data. *Genetics*, *155*, 945–59.
831 Roe, A., MacQuarrie, C., Gros-Louis, M. et al. (2014). Fitness dynamics within a poplar hybrid
832 zone: I. Prezygotic and postzygotic barriers impacting a native poplar hybrid stand.
833 *Ecology and Evolution*, *4*, 1629–1647. doi:10.1002/ece3.1029
834 Ross, R.I. (2010). Local adaptation and adaptive divergence in a hybrid species complex in
835 *Senecio* (Unpublished doctoral dissertation). Univeristy of Oxford.
836 Russello, M. A., Waterhouse, M. D., Etter, P. D., & Johnson, E. A. (2015). From promise to
837 practice: pairing non-invasive sampling with genomics in conservation. *PeerJ*, *3*, e1106.
838 doi:10.7717/peerj.1106
839 Schneider, C. A., Rasband, W. S., & Eliceiri, K. W. (2012). NIH Image to ImageJ: 25 years of
840 image analysis. *Nature Methods*, *9*, nmeth.2089. doi:10.1038/nmeth.2089
841 Scotti-Saintagne, C., Mariette, S., Porth, I. et al. (2004). Genome Scanning for Interspecific
842 Differentiation Between Two Closely Related Oak Species [*Quercus robur* L. and *Q.*
843 *petraea* (Matt.) Liebl.]. *Genetics*, *168*, 1615–1626. doi:10.1534/genetics.104.026849
844 Seehausen, O., Butlin, R. K., Keller, I., Wagner, C. E., Boughman, J. W., Hohenlohe, P. A., …
845 Saetre, G.-P. (2014). Genomics and the origin of species. *Nature Reviews Genetics*, *15*,
846 176–192. doi:10.1038/nrg3644
847 senecioDB. (undated). senecioDB: A genomic resource for *Senecio* species. Retrieved from
848 http://www.seneciodb.org/wordpress/?page_id=22.
849 Singhal, S., & Moritz, C. (2012). Strong selection against hybrids maintains a narrow contact
850 zone between morphologically cryptic lineages in a rainforest lizard. *Evolution*, *66*(5),
851 1474–1489. doi.org/10.1111/j.1558-5646.2011.01539.x
852 Sobel, J., Stankowski, S., Streisfeld, M. (2019). Variation in ecophysiological traits might
853 contribute to ecogeographic isolation and divergence between parapatric ecotypes of
854 *Mimulus aurantiacus*. *Journal of Evolutionary Biology*, *32*, 604–618.
855 doi:10.1111/jeb.13442
856 Stankowski, S., Sobel, J. M., & Streisfeld, M. A. (2017). Geographic cline analysis as a tool for
857 studying genome-wide variation: a case study of pollinator-mediated divergence in a
858 monkeyflower. *Molecular ecology*, *26*, 107–122. doi:10.1111/mec.13645
859 Tavares, H., Whibley, A., Field, D. L., Bradley, D., Couchman, M., Copsey, L., … Coen, E. (2018).
860 Selection and gene flow shape genomic islands that control floral guides. *Proceedings of*
861 *the National Academy of Sciences*, *115*(43), 201801832. doi:10.1073/pnas.1801832115

Teeter, K. C., Payseur, B. A., Harris, L. W., Bakewell, M. A., Thibodeau, L. M., O'Brien, J. E., … Tucker, P. K. (2008). Genome-wide patterns of gene flow across a house mouse hybrid zone. *Genome Research*, *18*, 67–76. doi:10.1101/gr.6757907

Tine, M., Kuhl, H., Gagnaire, P.-A., Louro, B., Desmarais, E., Martins, R., … Reinhardt, R. (2014). European sea bass genome and its variation provide insights into adaptation to euryhalinity and speciation. *Nature Communications*, *5*, 5770. doi:10.1038/ncomms6770

van Riemsdijk, I., Butlin, R. K., Wielstra, B., & Arntzen, J. W. (2019). Testing an hypothesis of hybrid zone movement for toads in France. *Molecular Ecology*, *28*(5), 1070-1083 doi:10.1111/mec.15005

Via, S. (2009). Natural selection in action during speciation. *Proceedings of the National Academy of Sciences*, *106*(Supplement 1), 9939–9946. doi:10.1073/pnas.0901397106

Vines, T., Dalziel, A., Albert, A., Veen, T., Schulte, P., & Schluter, D. (2016). Cline coupling and uncoupling in a stickleback hybrid zone. *Evolution*, *70*(5), 1023–1038. doi.org/10.1111/evo.12917

Wielstra, B., Burke, T., Butlin, R., Avcı, A., Üzüm, N., Bozkurt, E., … Arntzen, J. (2017). A genomic footprint of hybrid zone movement in crested newts. *Evolution Letters, 1*(2), 93–101. doi:10.1002/evl3.9

Willett, C. S. (2010). Potential fitness trade-offs for thermal tolerance in the intertidal copepod *Tigriopis californicus*. *Evolution, 64*, 2521–2534. doi:10.1111/j.1558-5646.2010.01008.x

Wu, C. (2001). The genic view of the process of speciation. *Journal of Evolutionary Biology*, *14*, 851–865. doi:10.1046/j.1420-9101.2001.00335.x

Young, N. D. (1996). Concordance and discordance: a tale of two hybrid zones in the pacific coast irises (Iridaceae). *American Journal of Botany*, *83*(12), 1623–1629. doi:10.1002/j.1537-2197.1996.tb12820.x

Data Accessibility Statement

All sequences were submitted to GenBank under the BioProject PRJNA546528. Genotypes used in estimating selection are available in Supplementary Information. Analytical input files and scripts for previously unpublished models in *dadi* are available through: https://github.com/edgarwly.

Author Contributions

DAF conceived and supervised the project. OGO and ASTP collected the samples and prepared them for sequencing. DAF measured leaf morphology. ELYW analysed the data with help from BN. ELYW wrote the draft of the manuscript, and all authors contributed to revisions.

Tables and Figures

Table 1. Recent studies estimating selection in hybrid zones using the approach of Barton & Gale (1993) using, ranked from highest to lowest estimates of selection strength.

Common name	Species	No. of loci	Selection estimates (CI)	Reference
Selection estimated using $s = 8\sigma^2/w^2$ (where σ = dispersal rate and w = cline width):				
Salamander	*Ensatina eschscholtzii*	9	0.46 - 0.75 (NA)	Alexandrino et al., 2005
Rainforest skink	*Carlia rubrigularis* (N & S lineages)	9	0.50 – 0.70 (NA)	Phillips et al., 2004
			0.22 – 0.49 (NA)	
Rainforest lizard	*Lampropholis coggeri* (C & S lineages)	11	0.403 (0.106 – 0.653)	Singhal & Moritz, 2012
Swainson's thrush	*Catharus ustulatus ustulatus* & *C. u. swainsoni*	3	0.19 – 0.40 (NA)	Delmore & Irwin, 2014
European rabbit	*Oryctolagus cuniculus cuniculus* & *O. c. algirus*	28	0.20 (0.05 – 0.64)	Carneiro et al., 2013
Morabine grasshopper	*Vandiemenella viatical* (2 chromosomal races)	10	0.197 (0.058 – 0.405)	Kawakami, Butlin, Adams, Paull, & Cooper, 2009
Yellow-rumped warbler	*Dendroica coronata coronata* & *D. c. auduboni*	2	0.18 (0.08 – 0.28)	Brelsford & Irwin, 2009
Ragwort	*Senecio aethnensis* & *S. chrysanthemifolius*	13	0.02 – 0.11 (NA)	Brennan et al., 2009
Common shrew	*Sorex araneus* (2 chromosomal races)	9	0.001 – 0.110 (NA)	Polyakov, White, Jones, Borodin, & Searle, 2011
		3	0.0003 – 0.003 (NA)	
House mouse	*Mus musculus musculus* & *M. m. domestica*	7	0.028 – 0.049 (NA)	Macholn et al., 2007
Red-backed fairy-wren	*Malurus melanocephalus melanocephalus* & *M. m. cruentatus*	102	0.007 (0.002 – 0.03)	Baldassarre, White, Karubian, & Webster, 2014
Selection estimated using $s = 4\sigma^2/w^2$:				
Crested Newt	*Triturus anatolicus* & *T. ivanbureschi*	49	0.11 (0.004 – 0.019)	Wielstra et al., 2017
Italian/ House sparrow	*Passer italiae* & *P. domesticus*	4	0.062 (0.038 – 0.109)	Bailey, Tesaker, Trier, & Sætre, 2015
Common/ Spined toad	*Bufo budo* & *B. spinosus*	32	0.0017 (0.0001 – 0.004)	van Riemsdijk et al. 2019
Selection estimated using $s = 3\sigma^2/w^2$:				
Stickleback	*Gasterostens aculeatus* (stream & anadromous ecotype)	7	0.097 (NA)	Vines et al., 2016
Marine gastropod	*Littorina saxatilis* (crab & wave ecotype)	57	0.06 (0.005 – 0.32)	Hollander, Galindo, & Butlin, 2015

	69	0.008 (NA)

904

905 **Table 2.** Distribution of molecular variation at the individual, population and species/hybrid
906 group levels (AMOVA). Only individuals used in demographic modelling were included.

	df	Sum of squares	Variance component	% of variation
Among species/hybrid groups	3	25475.50	239.74	37.06
Among populations	8	5270.24	25.66	3.97
Among individuals	119	45403.84	381.55	58.98
Total	130	76149.586	646.949	100

Pops	Model	No. of free param.	*dadi* log-likelihood	theta	AIC AIC	ΔAIC	Rel.likelihood	LRT 2ΔLL	P-value	N_1	N_2	T	s	P
C/A	eSplitExpMig	6	-197.31	392.91	406.62	7.54	0.0230			0.20	0.25	0.83	0.29	
	SplitExpMig	5	-198.70	540.87	407.39	8.32	0.0156			0.15	0.22	0.99		
	split_mig	4	-198.61	616.79	405.23	6.15	0.0462			0.13	0.20	1.10		
	split	3	-264.45	367.97	534.91	135.83	0.0000	131.68*	1.76E-30	0.28	0.28	0.23		
	IMpre	8	-196.96	216.71	409.92	10.85	0.0044			0.38	0.42	4.05	0.34	
	IM	6	-197.52	476.12	407.03	7.96	0.0187	1.11	0.57	0.15	0.16	0.66	0.33	
	IM1	5	-223.52	404.69	457.04	57.96	0.0000	52.00*	5.55E-13	0.16	0.20	0.35	0.65	
	IM2	5	-230.70	358.62	471.40	72.33	0.0000	66.37*	3.74E-16	0.19	0.35	0.40	0.21	
	IM2M	***7***	***-192.54***	***433.13***	***399.07***	***0***	***1***			***0.20****(0.18-0.22)*	***0.21****(0.17-0.25)*	***0.70****(0.45-0.95)*	***0.14****(0.12-0.17)*	***0.42****(0.33-0.52)*
	IM2M_1	5	-197.56	411.37	405.13	6.05	0.0485	10.05*	0.0066	0.18	0.25	0.98	0.35	
	SC	6	-212.66	182.06	437.32	38.25	0.0000			0.41	0.52			
	eSC	7	-196.45	384.47	406.89	7.82	0.0201			0.18	0.13		0.30	
	SC_IM2M	***8***	***-191.57***	***372.96***	***399.14***	***0.07***	***0.9666***			***0.22****(0.22-0.23)*	***0.10****(0.10-0.10)*		***0.23****(0.22-0.24)*	***0.26****(0.20-0.32)*
	IM2M_AL_SC	11	-194.14	290.02	410.27	11.20	0.0037			0.25	0.23		0.27	0.23
C/LH	IM	6	-246.61	293.92						0.41	0.82	4.55	0.44	
	IM2M	7	-253.23	297.13						0.27	0.88	3.52	0.31	0.13
C/HH	IM	6	-194.68	382.58						0.26	0.23	0.50	0.18	
	IM2M	7	-198.61	366.80						0.26	0.27	0.42	0.07	0.43
A/LH	IM	6	-234.40	506.69						0.25	0.24	2.19	0.58	
	IM2M	7	-222.65	404.34						0.31	0.24	0.66	0.26	0.03
A/HH	IM	6	-173.99	333.27						0.44	0.37	1.02	0.42	
	IM2M	7	-165.41	355.74						0.39	0.33	0.37	0.10	0.11
HH/LH	IM	6	-219.19	397.19						0.30	0.33	1.43	0.31	

IM2M	7	-218.61	358.97		0.32	0.34	0.71	0.41	0.64

Table 3. The likelihood of each demographic model investigated in *dadi* for each species/species or species/hybrid pair, results of likelihood ratio test (LTR) for certain nested models, Akaike information criterion (AIC) scores, ΔAIC scores (relative to best model), and the relative likelihood of each model compared with the best model, and their respective parameter estimate.

910 **Table 3.** (continued)

Pops	Model	M_A	M_B	M_C	M_D	M_{12}	M_{21}	M_S	M_E	M	T_a	T_s	T_m	T_{pre}	N_{pre}
C/A	eSplitExpMig							0.41	0.75						
	SplitExpMig							0.93	1.01						
	split_mig									1.14					
	split									0†					
	IMpre					0.31	0.53							0.22	4.31
	IM					0.76	1.24								
	IM1					0†	1.03								
	IM2					0.62	0†								
	IM2M	***0.31****(0.29-0.33)*	***1.36****(0.12-0.15)*												
	IM2M_1	0.74	0†												
	SC					0.42	0.63				3.04	0.83			
	eSC					0.62	0.77				0.31	0.64			
	SC_IM2M	***2.23****(0.22-0.23)*	***0.45****(0.42-0.48)*								***0.38****(0.37-0.39)*	***0.46****(0.44-0.48)*			
	IM2M_AL_SC	1.93	0.45	2.34	0.16						0.18	3.86	4.25		
C/LH	IM					1.73	3.74								
	IM2M	1.47	3.31												
C/HH	IM					0.77	2.33								
	IM2M	0.86	1.97												
A/LH	IM					1.28	2.01								
	IM2M	0.98	3.41												
A/HH	IM					1.73	4.09								
	IM2M	0.55	4.70												
HH/LH	IM					3.72	3.04								
	IM2M	3.61	2.26												

Remarks: under the 'Pops' column: C = *S. chrysanthemifolius*; LH = low-elevation hybrids; HH = high-elevation hybrids; A = *S. aethnensis*; the two best-fitting models are in bold and italic; in all cases, likelihood ratio tests are for the comparison with the model immediately above except for IM2, which is for comparison with IM*;* Under 'LRT', * indicates significant value; †indicates fixed value of parameters. Values in brackets for the models *IM2M* and *SC_IM2M* are confidence intervals obtained from bootstrapping. Refer to Figure S2 for definitions of parameters.

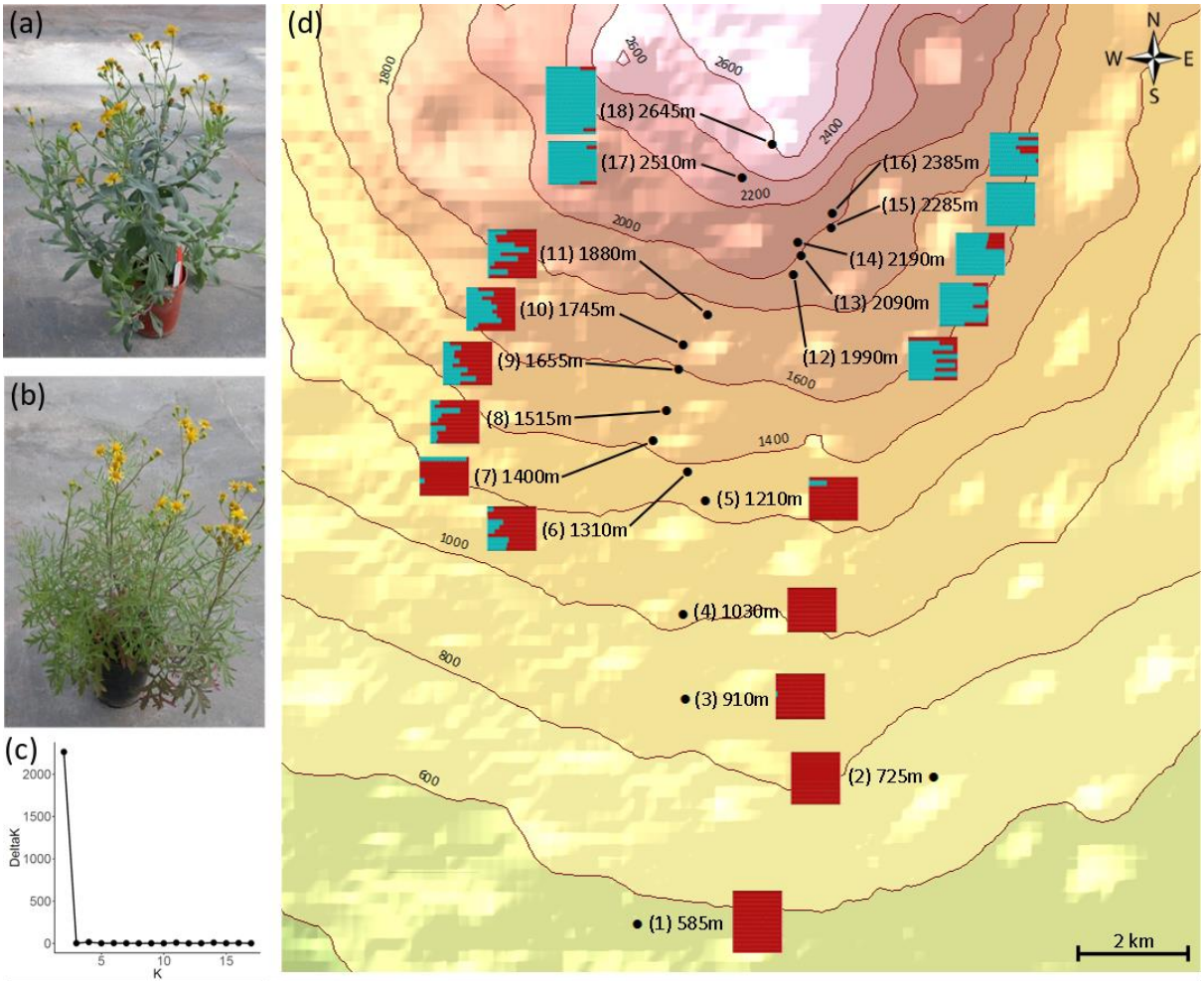

Figure 1. Distribution of sampled populations on Mount Etna and their genetic structure. (a) Photo of the high-elevation species *Senecio aethnensis* (obtained from senecioDB, undated). (b) Photo of the low-elevation species *Senecio chrysanthemifolius* (obtained from senecioDB, undated). (c) ΔK plot showing optimal K = 2. (d) Contour map showing the southern side of Mount Etna using Google Earth Pro (Google) and ArcGIS (ESRI). Each black dot represents a sampled site. Numbers in brackets represent population numbers and numbers next to them are elevations where they were sampled. Coloured rectangular plots next to each site represent its corresponding section in the *STRUCTURE* plot (using 1,769 nextRAD markers with less than 50% missing data and K = 2).

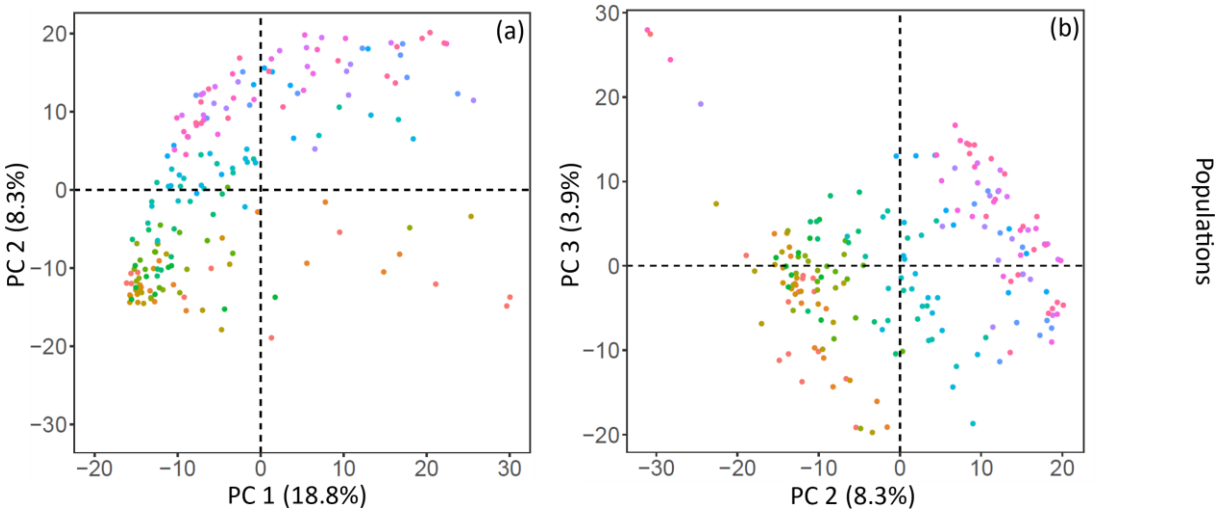

Figure 2. Plots from principle component analysis using 1,769 SNPs with less than 50% missing data. (a) PC 1 and 2. (b) PC 2 and 3. Points beyond -30 in both axes in (a) were not shown to allow comparable axis scales with (b). Full graph available in Figure S8.

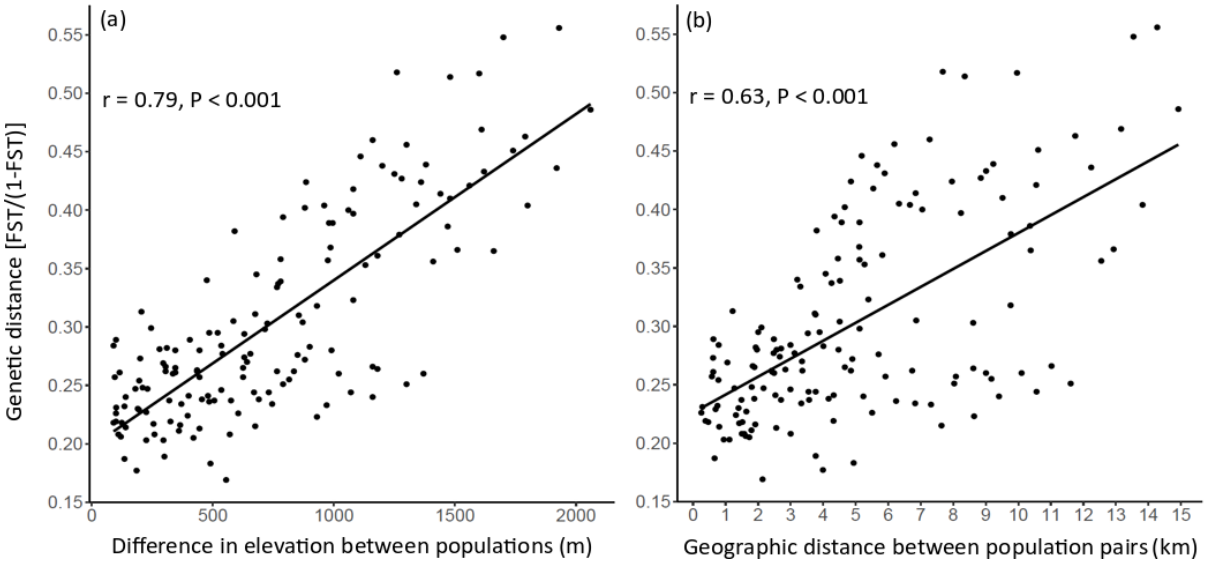

923 **Figure 3.** Mantel test for genetic distance, $F_{ST}/(1-F_{ST})$ and (a) difference in elevation between
924 population pairs; (b) geographic distance between population pairs.

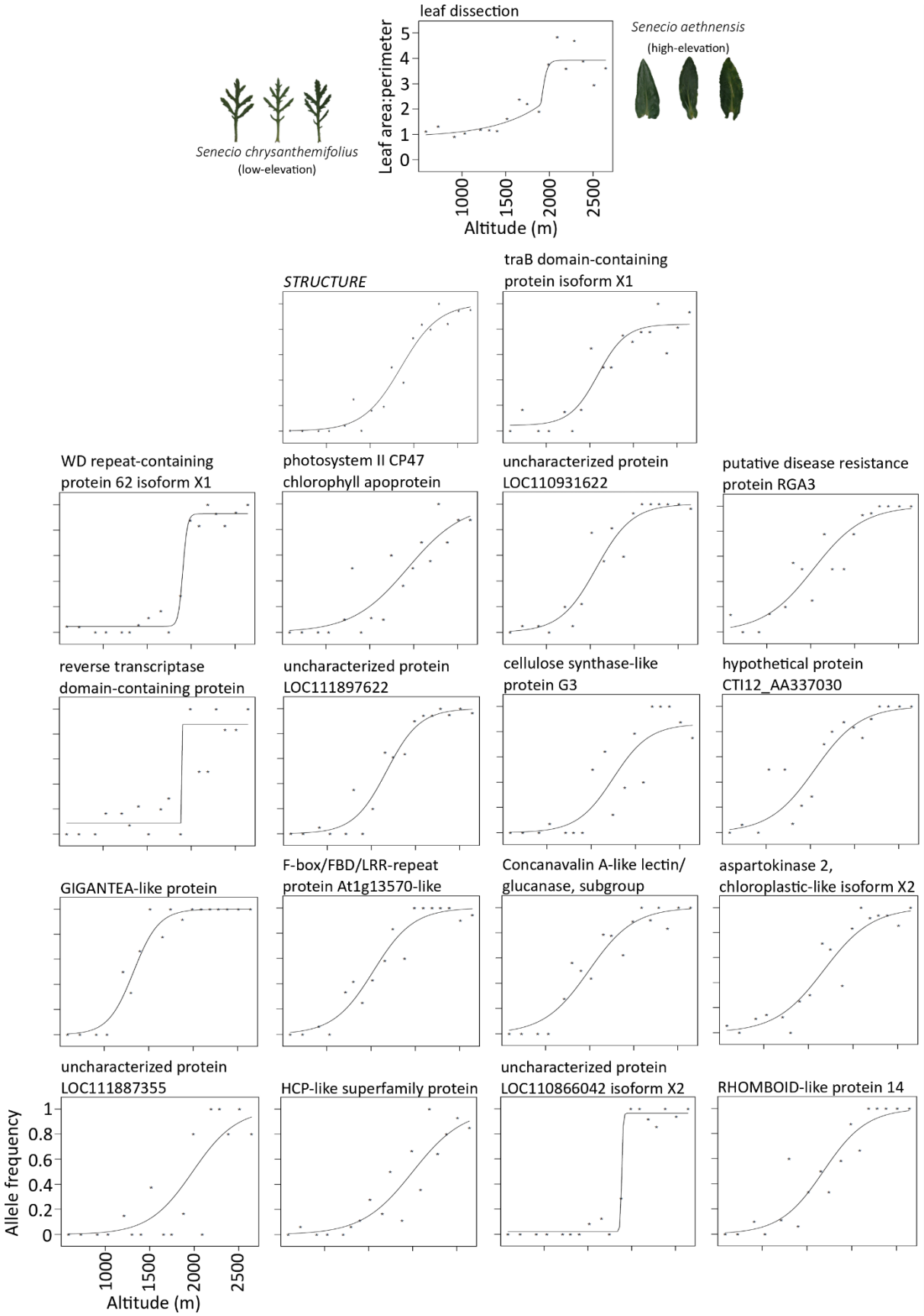

925 **Figure 4.** Clines for leaf dissection, *STRUCTURE*, and allele frequencies at 17 outlier SNPs

located in genes with functional annotation available (see Table S3 for details). Each asterisk in the plots represents mean trait value, ancestry score, or allele frequency for each population. Examples of leaf shape of each species are shown next to the leaf dissection cline.

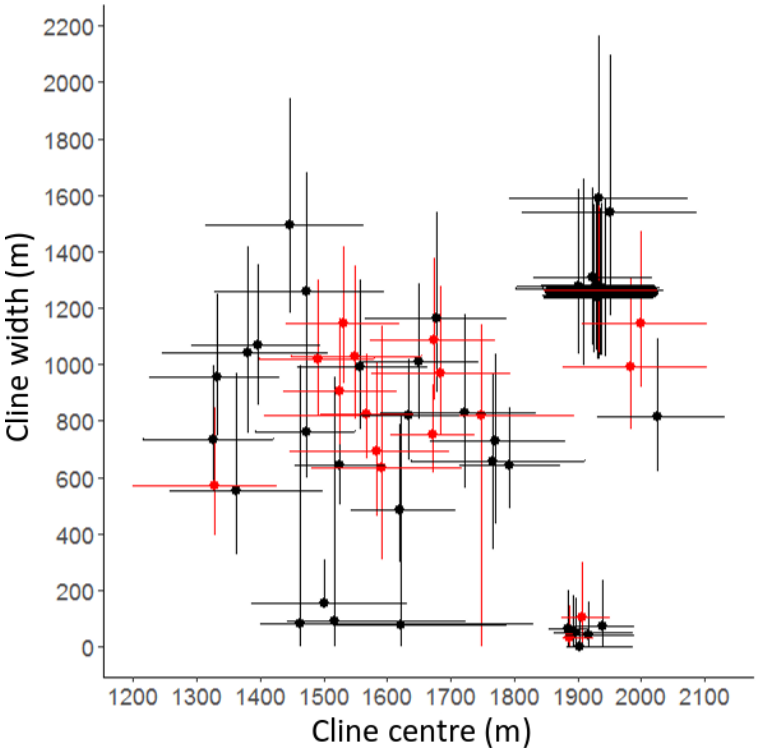

Figure 5. Variable cline coincidence and concordance of outlier clines. Maximum likelihood-estimated cline widths and cline centres of each outlier SNP are plotted as dots, while support limits are plotted as lines extending from the dots. Black and red data points represent non-outlier and outlier SNPs respectively. Refer to Table S4 for test results.

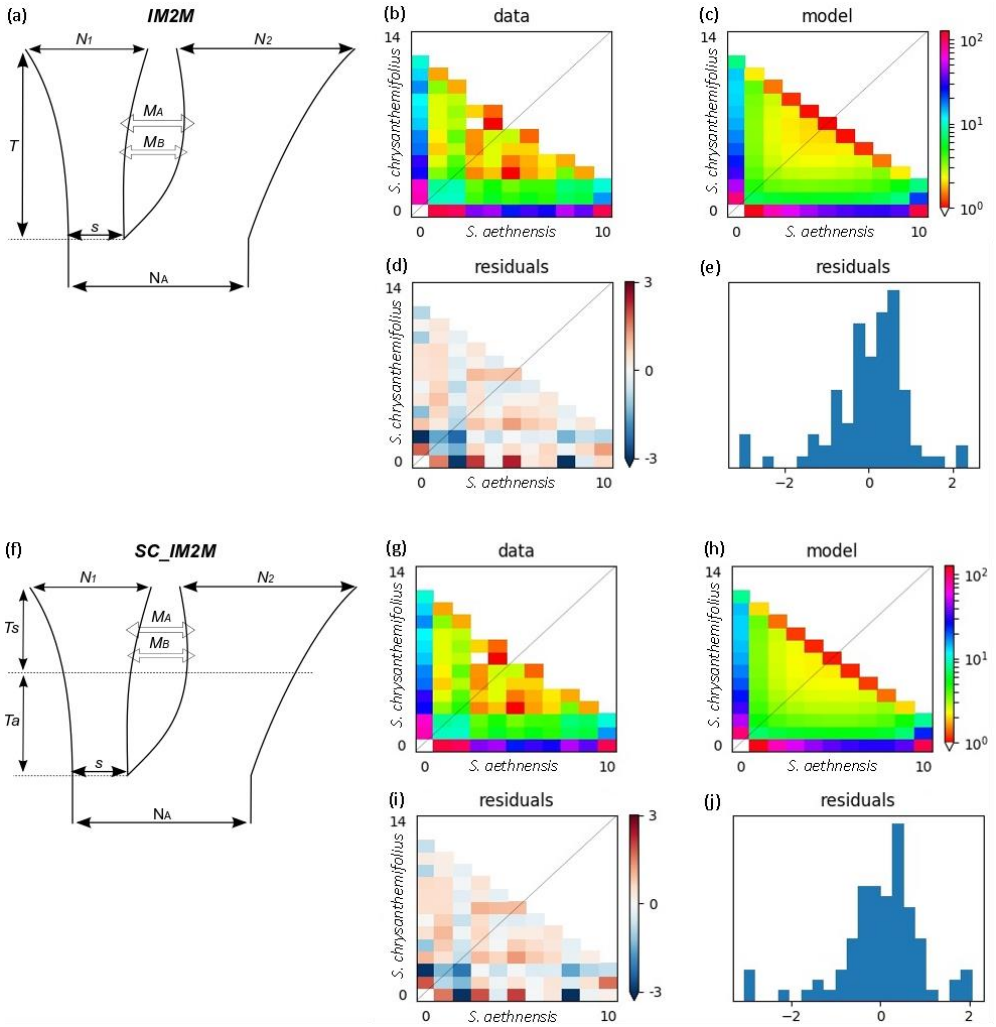

933 **Figure 6.** The fit of the two best demographic model (*IM2M* and *SC_IM2M*) to site frequency
934 spectrum data for *S. aethnensis* and *S. chrysanthemifolius*. (a) and (f) Schematic
935 representation of the two best demographic model. Each model has four corresponding
936 figures each: (b)-(e) for *IM2M* and (g)-(j) for *SC_IM2M*. (b) and (g) Observed two-dimensional
937 site-frequency-spectrum (2D-SFS). (c) and (h) 2D-SFS expected under the respective model.
938 (d)-(e), (i)-(j) Residuals between the observed and the expected site-frequency-spectra.